

Minimal Peptide Motif for Non-covalent Peptide–Heparin Hydrogels

Robert Wieduwild,[†] Mikhail Tsurkan,[‡] Karolina Chwalek,[‡] Priyanka Murawala,[†] Mirko Nowak,[‡] Uwe Freudenberg,[‡] Christoph Neinhuis,^{†,||} Carsten Werner,^{*,†,‡} and Yixin Zhang^{*,†}

[†]B CUBE Center for Molecular Bioengineering, Technische Universität Dresden, Arnoldstrasse 18, 01307 Dresden, Germany

[‡]Max Bergmann Centre of Biomaterials, Leibniz Institute of Polymer Research Dresden, Hohe Strasse 6, 01069, Dresden, Germany

^{||}Institute of Botany, Technische Universität Dresden, Zellescher Weg 20b, 01062 Dresden, Germany

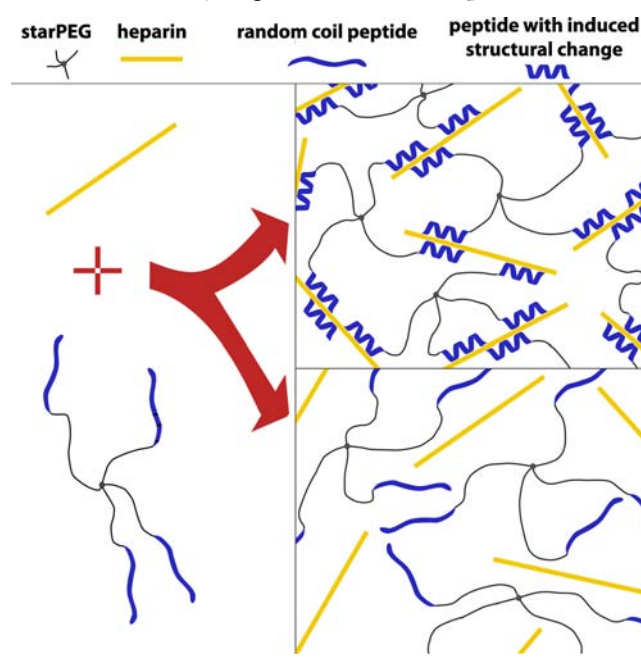
S Supporting Information

ABSTRACT: Reduction of complexity of the extracellular matrix (ECM) to a non-covalent structure with minimal chemically defined components represents an attractive avenue for understanding the biology of the ECM. The resulting system could lead to the design of tailor-made biomaterials that incorporate varying functionalities. Negatively charged glycosaminoglycans are the major components of the ECM. Their interaction with positively charged proteins is important for dynamic three-dimensional scaffold formation and function. We designed and screened minimal peptide motifs whose conjugates with polyethylene glycol interact with heparin to form non-covalent hydrogels. Here we show the structure/function relationship of the (RA)_n and (KA)_n motifs and determined that both basic residues and the heparin-induced α -helix formation are important for the assembly process. Simple rules allowed us to tune various aspects of the matrix system such as the gelation rates, biodegradability, rheological properties, and biofunctionality. The hydrogels can encapsulate cells and support cell survival.

Simple peptide motifs, which can be easily repeated and readily mutated to alter their binding properties to a particular biomolecule, are highly useful in the fields of chemical biology, biotechnology, and biomaterials. A system based on peptide motifs can be used to design tunable, non-covalent polymer matrices. Networks based on highly sulfated glycosaminoglycans such as heparin are of particular interest because their high, negative net charge results in an ability to bind to a plethora of important signaling molecules.¹ For this reason heparin has been used as a bioactive building block for modular, covalently cross-linked hydrogels that facilitate cell replacement therapies.²

In a non-covalent matrix system, the concentrations of the pair of interacting moieties are in the millimolar range. Thus, many known interacting pairs, e.g., protein/ligand,³ protein/protein,^{3b,4} oligosaccharide/protein,^{3b,5} or oligosaccharide/peptide⁶ pairs, could be used to design non-covalent hydrogels. However, the network structure is also an essential determinant of whether an interaction leads to the formation of small particles, aggregates, or a hydrogel. For example, the engineering of two distinct interacting pairs that control the network topology of protein hydrogels can dramatically decrease the hydrogel erosion rate.⁴ The heparin-binding antithrombin III (ATIII) peptide⁷

Scheme 1. Screening of Peptide Motifs Coupled to StarPEGs That Can Form Hydrogels with 14 kDa Heparin



and low-molecular-weight heparin can form a soft hydrogel when both molecules are conjugated to starPEG,^{6a,c} whereas the mixture of ATIII–starPEG conjugate and heparin aggregates form a pellet (Table 1). We speculated that the screening of peptide–polymer conjugates for their ability to form hydrogels with heparin could provide insight into the structure/function (S/F) relationships of the entire extracellular matrix. An understanding of the basic chemical and structural elements that affect the formation of this type of non-covalent network could allow the production of a simple non-covalent system with a broad range of tunability.

The heparin-binding domain of ATIII, which is the most studied of the heparin-binding peptides,⁸ undergoes a structural change to an α -helix upon heparin binding.⁷ Thus, we considered the possibility that α -helix formation and positively charged residues might be two key properties of a minimal heparin-interacting motif. A library of peptides was synthesized on the

Received: December 10, 2012

Published: February 6, 2013

Table 1. Hydrogel Formation of Peptide–StarPEG Conjugates with 14 kDa Heparin^a

peptide	peptide sequence	peptide–starPEG conjugate ^b [mM]	deformation speed ^c [g]	penetration speed ^c [g]	cell culture medium ^c
ATIII	CWGGKAFAKLAARLYRKA	5	N.D. ^d	N.D. ^d	formed ^d
KA5	CWGGKAKAKAKAKA	5	1144 ± 486	2162 ± 223	formed
KA7	CWGGKAKAKAKAKAKA	2.5	4485 ± 320	7419 ± 706	formed
KA7	CWGGKAKAKAKAKAKA	5	>15,119	>14,161 ± 1659	formed
RA7	CWGGRRARARARARA	5	109 ± 59	199 ± 50	formed
RA5	CWGGRRARARARARA	5	<70	<70	N.D.

^aRefer to Table S1 for the full table. ^bAll the peptides are linked to a 10 kDa starPEG. Hydrogel formation was tested in a 50- μ L mixture of 5 mM heparin and 5 mM (or 2.5 mM) of the starPEG–peptide conjugate in phosphate buffer (PBS), pH 7.4. ^cN.D. = not determined. ^dThe gel shrank.

basis of the repetition of the (BA)_n and (BG)_n motifs (where B is a basic residue, either arginine or lysine) (Table S1), and starPEG–peptide conjugates were screened for assembly with heparin (Scheme 1). (BA)_n peptides have a tendency to form α -helical structures.⁹ By contrast, (BG)_n peptides, which have the same charge densities as (BA)_n peptides, do not form helices because the glycine residues disrupt helix formation. Single BA motifs were used as negative controls because helix formation requires a minimum of five amino acids (for a Pauling–Corey–Branson α -helix).¹⁰ To determine the charge-density dependency of the interaction with heparin, the starPEG conjugates of (BBA)₅ and (BBG)₅ were synthesized and investigated.

Twenty-five peptides (Table 1) with an N-terminal CWGG sequence were synthesized by solid-phase peptide synthesis and purified by RP-HPLC (Figure S1). The tryptophan residue facilitates UV detection and purification, whereas the two glycine residues act as a spacer between the putative heparin-binding peptides and the polymer. The thiol group of cysteine was used to couple the peptides to maleimide-functionalized 10 kDa starPEG by Michael-type addition reactions. The resulting peptide–starPEG conjugates were purified by dialysis. To test for hydrogel formation, these conjugates were mixed with 14 kDa heparin at a 1:1 ratio in physiological phosphate buffer (PBS) (Scheme 1, Figures S3 and S4). To our knowledge, our library is the largest peptide–polymer conjugate library for studying the S/F relationship of oligosaccharide-dependent macromolecular non-covalent assembly.

Results of the hydrogel experiments are summarized in Tables 1 and S2. Mechanical properties of the obtained hydrogels were compared using two in-house developed screening methods. The deformation of the hydrogel and the penetration of metal beads were analyzed after applying different forces by centrifugation (Figure S4, Table 1). RA7–starPEG, KA5–starPEG, and KA7–starPEG formed stable hydrogels with heparin and had a wide range of stiffness levels (Table 1). No significant hydrogel swelling or loss of mass occurred during the experiments. RA5–starPEG (5 mM) and heparin (5 mM) formed a very soft hydrogel that could not be characterized by the centrifugation-based methods. Interestingly, the mechanical properties of these hydrogels could be further tuned by changing the concentrations of heparin and the peptide–starPEG conjugate (Table 1).

Electron microscopy images indicate that the peptide–starPEG conjugates and heparin assembled into micrometer-sized structures (Figure S12) that resembled those of covalent hydrogels with similar mechanical properties.¹¹ The KA7–starPEG, KA5–starPEG, and RA7–starPEG hydrogels were remarkably stable (Table S3). For example, the KA7–starPEG–heparin hydrogel could be kept in PBS and cell culture medium for months. The hydrogels were also resistant to harsh conditions such as DMSO, ethanol, 1 M HCl, 1 M NaOH, and saturated

NaCl. Because the hydrogels could be destroyed by TFE (trifluoroethanol), the non-covalent assembly is clearly dependent on the secondary structure of the peptide.

The (BA)_n amino acid motif was found to have a very simple S/F relationship through mutational studies in which “function” refers to the assembly of the peptide–starPEG conjugate and heparin into a hydrogel. This relationship is governed by the following rules: (1) At least five repeats of the (BA)_n motif are required for the assembly of the peptide–starPEG conjugate with heparin. Increasing the number of (BA)_n repeats results in stiffer gels (Table 1). Seven repeats of either the KA or RA motif produce stiffer hydrogels than do 5 repeats. If the same number of repeats is used, the (KA)_n peptides generate hydrogels that are stiffer than those from the (RA)_n peptides. (2) The heparin-induced α -helix formation is necessary for the assembly process (Figures 1a and S6d, Tables 1 and S2). None of the (BG)_n

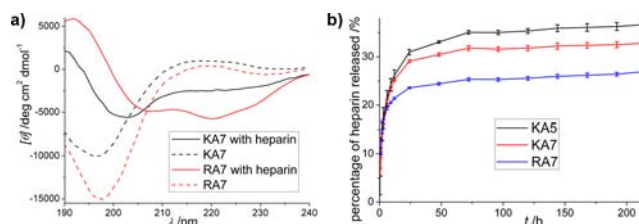


Figure 1. (a) Analysis of heparin-dependent peptide structural changes by CD. Both peptides exhibited a random coil structure. After adding 14 kDa heparin to a 2 \times molar concentration of the peptides, structural changes occurred. (b) Heparin release was assessed by mixing peptide–starPEG conjugates and 14 kDa heparin that had been labeled with TAMRA in 50 μ L of cell culture medium containing 2% fetal bovine serum (FBS) to a final concentration of 5 mM. A 200 μ L sample from the 1 mL of supernatant was analyzed, and the volume was replaced with 200 μ L of fresh medium.

sequences results in hydrogel formation, despite the fact that these sequences have the same number of positive charges as their (BA)_n counterparts. In addition, because the insertion of D-amino acids into an L-peptide can disrupt α -helix structure, replacing all of the L-lysines with D-lysine or all of the L-alanines with D-alanine in KA7–starPEG results in peptide–starPEG conjugates that cannot assemble with heparin to form a hydrogel. Furthermore, a single D-amino acid substitution in the KA7–starPEG completely abolishes hydrogel formation. Most interestingly, when both the L-lysines and the L-alanines in the KA7–starPEG are replaced with D-amino acids, hydrogel formation is observed. The all-D- and all-L-hydrogels have very similar mechanical properties (Figure S5). Due to the resistance of D-peptides to proteolysis, the D-peptide hydrogel system could be beneficial for long-term in vivo applications. (3) Higher charge densities do not necessarily produce a stronger hydrogel

(Tables 1 and S2). For example, KKA5, RRA5, KKG5, and RRG5 have higher charge densities than KA7, RA7, and KA5. However, the KKA5, KKG5, RRA5, and RRG5 conjugates and heparin do not form non-covalent hydrogels. (4) A highly sulfated oligosaccharide structure is required for gel formation, as desulfated heparin does not form a hydrogel with KA7–starPEG

In summary, the S/F relationship studies indicated that the gelation process is dependent not only on the positively charged peptides but also on the peptide conformations. To confirm this hypothesis, we used circular dichroism (CD) to study the structural changes of the heparin-binding peptides in the presence or absence of heparin (Figures 1a and S6). In the absence of heparin, (BG)_n, (BBG)_n, (BA)_n, and (BBA)_n formed random coil structures (Figures 1a and S6). In the presence of heparin KA7, KA5, RA7, and RA5 peptides experienced structural changes to α -helices (Figures 1a and S6b), whereas the BG5, BG7, and BBG5 peptides did not exhibit significant structural changes (Table S2). Interestingly, this observation correlated well with the hydrogel formation properties of the particular peptide–starPEG conjugates with heparin. RRA5 was the only peptide that formed an α -helix with heparin but did not form a hydrogel (Figure S6c). We speculate that the RRA5–starPEG conjugate does not possess an optimal charge distribution, which appears to be important for the interactions with the sulfate groups of heparin. As expected, ATIII produced a strong α -helix formation signal upon heparin binding (Figure S6f). Although ATIII–starPEG and heparin exhibited strong interactions, the mixture formed a pellet-like material with a solid content of \sim 50% (Table 1).

The peptide–starPEGs and heparin can cross-link the entire volume when the components are above certain concentrations. No gelation occurred when KA5–starPEG was lower than 4 mM in the presence of 5 mM heparin. Reducing the solid content could cause syneresis for the KA7–starPEG and RA7–starPEG hydrogels. For example, when [KA7–starPEG] is <2.0 mM in the presence of 0.5 mM heparin, the resulting hydrogel is smaller than the initial volume, leaving a layer of supernatant above the hydrogel. The syneresis effect reflects the minimum cross-linking density required for the non-covalent network.

To design a hydrogel suitable for cell embedding, gelation time is important. Due to the different charge properties of RA7–starPEG, KA7–starPEG, and KA5–starPEG, gelation times of each are different. RA7–starPEG and heparin formed a hydrogel instantly in PBS at a final concentration of 5 mM of each. Under the same conditions, heparin and KA7–starPEG or heparin and KA5–starPEG formed hydrogels more slowly. To follow the hydrogel formation process, we constructed an automated gelation probing device, which is connected to a balance that records the force generated by a needle–hydrogel contact (Figure S7). $T_{1/2}$ (the time to reach 50% of the maximal resistance) of 5 mM KA5–starPEG and 5 mM heparin at room temperature was \sim 3 h; $T_{1/2}$ for KA7–starPEG and heparin at similar conditions was 1 h (Figure S8a,c). Lower concentrations of both components prolonged the gelation time (Figure S8a,b). Temperature increases accelerated the gelation; e.g. at 37 °C, $T_{1/2}$ of 5 mM KA5–starPEG and 5 mM heparin was <1 h (data not shown).

Heparin is a widely used anticoagulant.¹² Therefore, heparin release might allow anti-thrombogenic action of hydrogels. To investigate heparin release we used fluorescently labeled heparin. Hydrogels were formed from TAMRA–heparin and KA5–starPEG, KA7–starPEG, or RA7–starPEG (Figure 1b) and were subsequently incubated in cell culture medium at 37 °C. After an

initial phase involving the release of 20% of the heparin within 10 h, a slow rate of heparin release was observed for the subsequent 9 days for all three hydrogels. In accordance with reports that heparin is more strongly bound by arginine-containing peptides than by their lysine counterparts,¹³ the RA7–starPEG hydrogel had the lowest release. Since KA5 has fewer positive charges than KA7, the release from KA5–starPEG hydrogels was higher than the release from KA7–starPEG hydrogels. Heparin release does not cause significant loss of hydrogel mass, and the non-covalent matrices are stable over a time period of months. We speculate that some heparin molecules that are not stably connected in the network can escape from the matrices.

To verify the wide range of mechanical properties of the non-covalent hydrogels, the bulk rheometric properties of the KA7–starPEG and KA5–starPEG conjugates with heparin were characterized by frequency and strain sweep experiments (Figure 2). The rheometric measurements confirmed that separate

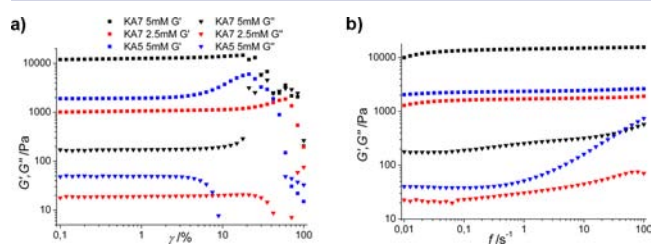


Figure 2. Bulk rheology of mixtures of peptide–starPEG conjugates and 14 kDa heparin. Each final mixture in PBS contained 5 mM of both the peptide–starPEG conjugate and heparin or 2.5 mM of the peptide–starPEG conjugate and 0.5 mM heparin. (a) Amplitude sweep with a frequency of 1 Hz. (b) Frequency sweep with a 2% deformation.

solutions of either heparin or peptide–starPEG conjugate do not exhibit any hydrogel-like mechanical properties (Figure S10a,b). For the assembling hydrogels, the storage modulus, G' , is orders of magnitude higher than the loss modulus G'' (\sim 2%) for all samples, a result indicative of strong and stable networks with the highly elastic nature that has also been observed in covalent hydrogel.^{2a} By changing the heparin and/or peptide–starPEG concentrations, the mechanical properties can be further tuned over more than an order of magnitude. Remarkably, at a concentration as low as 0.5 mM, heparin can still form a hydrogel with KA7–starPEG (2.5 mM).

Injectable hydrogels are important for biomedical applications. Injection can reduce the stiffness, while the mechanical properties could be recovered or become even stiffer than the untreated sample (Figure S9). We carried out two continuous rheological measurements on KA7–starPEG and KA5–starPEG hydrogels (Figure S11). As expected, moderate increases of G' were observed. These results indicate that mechanical stress can cause disturbance and rearrangement of the physically cross-linked matrices.

To test the applicability of the hydrogels for in situ cell encapsulation, we assessed the survival rate of human neonatal dermal fibroblasts (HDFn) that were exposed to individual components of the hydrogel. KA7–starPEG, KA5–starPEG, RA7–starPEG, or 14 kDa heparin had no toxic effects on the HDFn (Figure S13). The different gelation times of the peptide–starPEG conjugates with heparin allowed us to test the optimal conditions for cell encapsulation, resulting in the successful embedding of cells in KA7–starPEG- and KA5–starPEG-based hydrogels. The slow hydrogel formation of 5 mM KA5–starPEG or 2.5 mM KA7–starPEG with heparin resulted in inhomoge-

neous cell encapsulation (embedding in the bottom layer of the hydrogel was greater than in the upper layer). By contrast, because of the relatively rapid gelation, 5 mM KA7–starPEG and 5 mM heparin provided the optimal reagents for cell embedding.

Encapsulation of fibroblasts in all of the hydrogels produced no toxic effects. Cells that were encapsulated in the bulky hydrogels were alive and could metabolize 3-(4,5-dimethylthiazol-2-yl)-2,5-diphenyltetrazolium bromide (MTT) to produce purple formazan (Figure 3a). After one week of culture, the

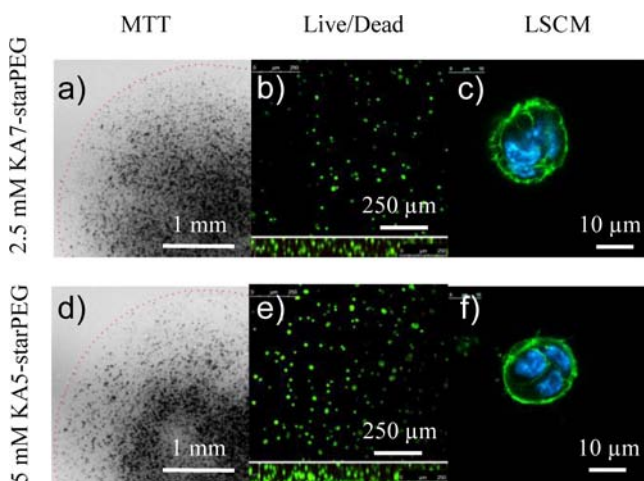


Figure 3. HDFNs embedded in hydrogels. Final mixtures in complete cell culture medium were (a–c) 5 mM KA5–starPEG conjugate and 14 kDa heparin and (d–f) 2.5 mM KA7–starPEG conjugate and 14 kDa heparin. Cell concentrations were 10^6 cells/mL. (a,d) MTT-stained HDFNs in the hydrogel (wide-field microscope). (b,c,e,f) Confocal laser scanning microscopy images. (b,e) Live/dead stained HDFNs (green, alive; red, dead) and z-stack (bottom): (b) $99 \pm 1\%$ alive, (e) $98 \pm 1\%$ alive. (c,f) Actin filaments and nuclei of HDFNs stained with phalloidin-CF488 (green) and DAPI (red), respectively.

live/dead assays indicated respectively that in the KA5–starPEG/heparin and KA7–starPEG/heparin hydrogels 99% and 98% of the cells were alive (Figure 3b). As shown in Figure 3c, many cell colonies derived from a single-cell suspension were observed in both hydrogels. The hydrogels do not support cell spreading very well, and the matrices are stable against proteolysis. These features can be improved in the future through incorporating peptide sequences sensitive to proteolytic activity¹⁴ or sequences such as RGD peptide to improve cell attachment.^{14b,c,15}

Herein we report a novel, non-covalent hydrogel system composed of heparin and peptide–starPEG conjugates. Simple variables govern a highly flexible system that can easily be tuned by changing the number of $(BA)_n$ repeats, by adjusting the concentration of each component, or by introducing simple mutations. Most importantly, stable hydrogels can be formed in the presence of large quantities of cells in cell culture medium at 37 °C, and cells embedded within the non-covalent hydrogel survive and are metabolically active. Studies of this versatile biomaterial are currently being extended by incorporating more functionalities, such as enzymatically cleavable¹⁴ or adhesive peptides.^{14b,c,15}

■ ASSOCIATED CONTENT

Supporting Information

Experimental procedures, chemical syntheses, high-throughput mechanical analysis, CD spectroscopy, stability and gelation time

analysis, electron microscope pictures, cell culture, and toxicity assays. This material is available free of charge via the Internet at <http://pubs.acs.org>.

■ AUTHOR INFORMATION

Corresponding Author

yixin.zhang@bcube-dresden.de; werner@ipfdd.de

Notes

The authors declare no competing financial interest.

■ ACKNOWLEDGMENTS

We thank Ulrike Hofmann, Peggy Berg, and Markus Günther for technical support. We thank Roland Vogel for help on rheometry (Leibniz Institute of Polymer Research Dresden) and Dr. Habil Martin Müller for help with CD spectroscopy measurements. R.W., P.M., and Y.Z. were supported by the Bundesministerium für Bildung und Forschung (BMBF) through Grant 03Z2EN12.

■ REFERENCES

- (1) Capila, I.; Linhardt, R. J. *Angew. Chem., Int. Ed.* **2002**, *41*, 390.
- (2) (a) Freudenberg, U.; Hermann, A.; Welzel, P. B.; Stirl, K.; Schwarz, S. C.; Grimmer, M.; Zieris, A.; Panyanuwat, W.; Zschoche, S.; Meinhold, D. *Biomaterials* **2009**, *30*, 5049. (b) Zieris, A.; Prokoph, S.; Levental, K. R.; Welzel, P. B.; Grimmer, M.; Freudenberg, U.; Werner, C. *Biomaterials* **2010**, *31*, 7985.
- (3) (a) Wong Po Foo, C. T. S.; Lee, J. S.; Mulyasmita, W.; Parisi-Amon, A.; Heilshorn, S. C. *Proc. Natl. Acad. Sci. U.S.A.* **2009**, *106*, 22067. (b) Wang, H.; Shi, Y.; Wang, L.; Yang, Z. *Chem. Soc. Rev.* **2013**, *42*, 891.
- (4) Yamaguchi, N.; Zhang, L.; Chae, B.-S.; Palla, C. S.; Furst, E. M.; Kiick, K. L. *J. Am. Chem. Soc.* **2007**, *129*, 3040.
- (5) Shen, W.; Zhang, K.; Kornfield, J. A.; Tirrell, D. A. *Nat. Mater.* **2006**, *5*, 153.
- (6) (a) Yamaguchi, N.; Chae, B.-S.; Zhang, L.; Kiick, K. L.; Furst, E. M. *Biomacromolecules* **2005**, *6*, 1931. (b) Yamaguchi, N.; Kiick, K. L. *Biomacromolecules* **2005**, *6*, 1921. (c) Zhang, L.; Furst, E. M.; Kiick, K. L. *J. Controlled Release* **2006**, *114*, 130. (d) Kiick, K. L. *Soft Matter* **2008**, *4*, 29. (e) Spinelli, F. J.; Kiick, K. L.; Furst, E. M. *Biomaterials* **2008**, *29*, 1299.
- (7) Tyler-Cross, R.; Harris, R. B.; Sobel, M.; Marques, D. *Protein Sci.* **1994**, *3*, 620.
- (8) (a) Jayaraman, G.; Wu, C. W.; Liu, Y. J.; Chien, K. Y.; Fang, J. C.; Lyu, P. C. *FEBS Lett.* **2000**, *482*, 154. (b) Verrecchio, A.; Germann, M. W.; Schick, B. P.; Kung, B.; Twardowski, T.; San Antonio, J. D. *J. Biol. Chem.* **2000**, *275*, 7701. (c) Rullo, A.; Nitz, M. *Biopolymers* **2010**, *93*, 290. (d) Wu, C. W.; Jayaraman, G.; Chien, K. Y.; Liu, Y. J.; Lyu, P. C. *Peptides* **2003**, *24*, 1853.
- (9) Nick Pace, C.; Martin Scholtz, J. *Biophys. J.* **1998**, *75*, 422.
- (10) Pauling, L.; Corey, R. B.; Branson, H. R. *Proc. Natl. Acad. Sci. U.S.A.* **1951**, *37*, 205.
- (11) Trappmann, B.; Gautrot, J. E.; Connelly, J. T.; Strange, D. G. T.; Li, Y.; Oyen, M. L.; Cohen Stuart, M. A.; Boehm, H.; Li, B.; Vogel, V.; Spatz, J. P.; Watt, F. M.; Huck, W. T. S. *Nat. Mater.* **2012**, *11*, 642.
- (12) Björk, I.; Lindahl, U. *Mol. Cell. Biochem.* **1982**, *48*, 161.
- (13) (a) Jackson, R. L.; Busch, S. J.; Cardin, A. D. *Physiol. Rev.* **1991**, *71*, 481. (b) Fromm, J. R.; Hileman, R. E.; Caldwell, E. E. O.; Weiler, J. M.; Linhardt, R. J. *Arch. Biochem. Biophys.* **1997**, *343*, 92. (c) Mascotti, D. P.; Lohman, T. M. *Biochemistry* **1995**, *34*, 2908.
- (14) (a) Seliktar, D.; Zisch, A. H.; Lutolf, M. P.; Wrana, J. L.; Hubbell, J. A. *J. Biomed. Mater. Res., Part A* **2004**, *68A*, 704. (b) Lutolf, M. P.; Hubbell, J. A. *Nat. Biotechnol.* **2005**, *23*, 47. (c) Tsurkan, M. V.; Chwalek, K.; Levental, K. R.; Freudenberg, U.; Werner, C. *Macromol. Rapid Commun.* **2010**, *31*, 1529. (d) Anderson, S. B.; Lin, C.-C.; Kuntzler, D. V.; Anseth, K. S. *Biomaterials* **2011**, *32*, 3564. (e) Chwalek, K.; Levental, K. R.; Tsurkan, M. V.; Zieris, A.; Freudenberg, U.; Werner, C. *Biomaterials* **2011**, *32*, 9649.
- (15) Benoit, D. S. W.; Durney, A. R.; Anseth, K. S. *Biomaterials* **2007**, *28*, 66.